Personalized Medicine and Imaging

Clinical Cancer Research

^{89}Zr-trastuzumab and ^{89}Zr-bevacizumab PET to Evaluate the Effect of the HSP90 Inhibitor NVP-AUY922 in Metastatic Breast Cancer Patients

Sietske B.M. Gaykema[1], Carolien P. Schröder[1], Joanna Vitfell-Rasmussen[5], Sue Chua[5], Thijs H. Oude Munnink[1], Adrienne H. Brouwers[2], Alfons H.H. Bongaerts[3], Mikhail Akimov[6,7], Cristina Fernandez-Ibarra[6,7], Marjolijn N. Lub-de Hooge[2,4], Elisabeth G.E. de Vries[1], Charles Swanton[5], and Udai Banerji[5]

Abstract

Purpose: HSP90 chaperones have key client proteins that are involved in all hallmarks of breast cancer growth and progression. The primary aim of this clinical trial was to evaluate the feasibility of using ^{89}Zr-trastuzumab PET (for HER2-positive breast cancer) or ^{89}Zr-bevacizumab PET [for estrogen receptor (ER)–positive breast cancer] to determine *in vivo* degradation of client proteins caused by the novel HSP90 inhibitor NVP-AUY922.

Experimental Design: Of note, 70 mg/m^2 NVP-AUY922 was administered intravenously in a weekly schedule to patients with advanced HER2 or ER-positive breast cancer. Biomarker analysis consisted of serial PET imaging with 2[18F]fluoro-2-deoxy-D-glucose (FDG), ^{89}Zr-trastuzumab, or ^{89}Zr-bevacizumab. Response evaluation was performed according to RECIST1.0. FDG, ^{89}Zr-trastuzumab, and ^{89}Zr-bevacizumab distributions were scored visually and quantitatively by calculating the maximum standardized uptake values (SUV_{max}). In blood samples, serial HSP70 levels, extracellular form of HER2 (HER2-ECD), and pharmacokinetic and pharmacodynamic parameters were measured.

Results: Sixteen patients (ten HER2-positive and six ER-positive tumors) were included. One partial response was observed; seven patients showed stable disease. SUV_{max} change in individual tumor lesions on baseline versus 3 weeks ^{89}Zr-trastuzumab PET was heterogeneous and related to size change on CT after 8 weeks treatment ($r^2 = 0.69$; $P = 0.006$). Tumor response on ^{89}Zr-bevacizumab PET and FDG-PET was not correlated with CT response.

Conclusions: NVP-AUY922 showed proof-of-concept clinical response in HER2-amplified metastatic breast cancer. Early change on ^{89}Zr-trastuzumab PET was positively associated with change in size of individual lesions assessed by CT. *Clin Cancer Res; 20(15); 3945–54. ©2014 AACR.*

Introduction

Metastatic breast cancer remains an incurable disease in the majority of cases, despite advances in systemic treatment that have improved median survival (1, 2). The development of novel agents for this disease is an area of unmet need. HSP90 is a molecular chaperone which plays a critical role in protein folding and function of a broad range of client proteins (3). HSP90 client proteins playing a role in metastatic breast cancer include HER2, the hypoxia-inducible factor-1α (HIF1α), and the estrogen receptor (ER; refs. 4–6). HER2 is a sensitive client protein of HSP90, which can be depleted by HSP90 inhibition with NVP-AUY922 in many different preclinical experiments including breast cancer models (7, 8). HIF1α is the key factor involved in upregulating the transcription of VEGF-A in hypoxic cells (9). HSP90 is overexpressed in metastatic breast cancer. In addition, HSP90 in tumor cells preferentially binds to HSP90 inhibitors compared with normal cells, which further validates HSP90 as a cancer target (10, 11). Thus, there are many different reasons for evaluating HSP90 inhibitors in breast cancer. Several HSP90 inhibitors are currently in clinical development. Of the resorcinyclic pyrazole/isoaxazole amide analogues, HSP90 inhibitor NVP-AUY922 is the most potent (8). NVP-AUY922 is active against HER2-positive as well as HER2-negative human breast cancer cells *in vitro* and

Authors' Affiliations: Departments of [1]Medical Oncology, [2]Nuclear Medicine and Molecular Imaging, [3]Radiology and [4]Hospital and Clinical Pharmacy, University of Groningen, University Medical Center Groningen, Groningen, the Netherlands, [5]Section of Medicine, UK and Drug Development Unit, The Institute of Cancer Research, The Royal Marsden Hospital, Sutton, United Kingdom; and [6]Novartis Pharma AG, Basel, Switzerland and [7]Novartis Pharmaceuticals, Cambridge, Massachusetts

Note: Supplementary data for this article are available at Clinical Cancer Research Online (http://clincancerres.aacrjournals.org/).

Corresponding Author: Carolien P. Schröder, Department of Medical Oncology, University Medical Center Groningen, PO Box 30001, 9700 RB Groningen, the Netherlands. Phone: 31-50-3616161; Fax: 31-50-3614862; E-mail: c.p.schroder@umcg.nl

doi: 10.1158/1078-0432.CCR-14-0491

Translational Relevance

Metastatic breast cancer is rarely cured, and finding treatment for this disease is an unmet clinical need. HSP90 is a target of interest in cancer treatment, as a molecular chaperone that plays a critical role in protein folding and thereby functioning of a broad range of cancer-related client proteins. Gaining insight of *in vivo* degradation of client proteins caused by HSP90 inhibition is challenging. In this clinical trial, the effect of HSP90 inhibitor NVP-AUY922 on client proteins HER2 or VEGF [with hypoxia-inducible transcription factor-1α (HIF1α) as the actual client protein] was studied with ^{89}Zr-trastuzumab PET or ^{89}Zr-bevacizumab PET, in patients with advanced HER2 or estrogen receptor-positive metastatic breast cancer. The results of PET imaging were correlated with conventional CT scanning. ^{89}Zr-trastuzumab uptake on PET at 3 weeks correlated with CT responses in individual lesions at 8 weeks and revealed areas of heterogeneous response in patients with HER2-amplified metastatic breast cancer. Thus, novel PET probes such as ^{89}Zr-trastuzumab can be used to provide insights into responses to novel agents active in HER2-amplified breast cancer such as NVP-AUY922.

in vivo (8, 12, 13). Clinical responses to HSP90 inhibitors have been shown in multiple early-phase studies (14–16). Furthermore, HSP90 inhibition has shown efficacy when used in conjunction with other HER2-targeting agents such as trastuzumab (17). Nonetheless, gaining insight into the *in vivo* degradation of client proteins caused by HSP90 inhibition is challenging.

In this setting, *in vivo* visualization of HSP90 inhibition effect might be helpful. 2[18F]fluoro-2-deoxy-D-glucose (FDG)- PET for assessing tumor glucose metabolism, is used to monitor early drug response to anticancer agents (18–21). More target-based imaging of HSP90 inhibition effect was performed in preclinical studies, in which critical client proteins VEGF and HER2 could be visualized with zirconium-89 (^{89}Zr)-bevacizumab PET, gallium-68-(Fab'2) trastuzumab PET, and ^{89}Zr-trastuzumab PET imaging (22–24). In human breast cancer xenograft mouse model models, tumor uptake of ^{18}F-FDG was unaffected by treatment with the HSP90 inhibitor 17-*N*-allylamino-17-demethoxygeldanamycin (17AAG), whereas radiolabeled trastuzumab tumor uptake was on average reduced by 50%. This indicates that target-based imaging may be more useful as an early biomarker for HSP90 inhibition than metabolic ^{18}F-FDG imaging (24). ^{89}Zr-trastuzumab PET and ^{89}Zr-bevacizumab PET has been used in several clinical trials, including in breast cancer–specific studies (25–27).

To evaluate HSP90 inhibition effect on the *in vivo* degradation of client proteins, blood-based assays have been used. Serial circulating HER2 extracellular domain (HER2-ECD) measurements predicted response to trastuzumab-based therapy in a study of 55 patients (28). In a phase I study with NVP-AUY922, plasma NVP-AUY922 levels and pharmacodynamic biomarkers such as HSP70 induction in peripheral blood mononuclear cells (PBMC) were assessed, in addition to establishment of the toxicity profile (29).

Thus, the primary aim of this clinical trial with HSP90 inhibitor NVP-AUY922 in HER2- or ER-positive metastatic breast cancer patients was to evaluate the feasibility of using serial FDG-PET and novel ^{89}Zr-trastuzumab PET or ^{89}Zr-bevacizumab PET to determine the *in vivo* degradation of client proteins caused by the HSP90 inhibitor NVP-AUY922. Furthermore, we aimed to evaluate whether these assessments were related to CT response (according to RECIST) and serum shed HER2 levels (if applicable), and to underpin these assessments with evidence of pharmacokinetic and pharmacodynamic parameters which have already been defined in detail in the previous phase I study (29).

Patients and Methods

Patients

Eligible patients for treatment with NVP-AUY922, had a diagnosis of histologically confirmed, measurable progressive metastatic or locally advanced breast cancer, and had received up to two prior lines of cytotoxic therapy for advanced disease. In addition, patients with HER2-positive breast cancer were required to have a history of trastuzumab resistance and up to a maximum of three anti-HER2–based regimens for advanced disease. Patients with ER-positive breast cancer had progressive disease on at least one and up to a maximum of three lines of standard endocrine therapy. Further eligibility criteria included: age $\geq$18 years, World Health Organisation (WHO) performance status $\leq$2, at least one measurable lesion evaluable with RECIST1.0 (30), HER2-positive (IHC) 3+ or FISH ratio $\geq$2, or ER-positive breast cancer (archival primary tumor tissue), and resolution of toxicities from other therapies to National Cancer Institute common terminology criteria for adverse events (NCI CTCAE version 3.0; Bethesda, MA) grade $\leq$2. Patients should have adequate hematologic, hepatic, and renal function that was defined by laboratory values, adequate cardiac function defined by electrocardiography and multi gated acquisition scan (MUGA) scan or ultrasound. Patients eligible for treatment with NVP-AUY922 in this trial (Trial Registration ID: NCT00526045) were also eligible for assessment of treatment effect with ^{89}Zr-trastuzumab PET (Trial Registration ID: NCT01081600) for HER2-positive breast cancer or ^{89}Zr-bevacizumab PET (Trial Registration ID: NCT01081613) for ER-positive breast cancer. This clinical trial was performed at the University Medical Center of Groningen (Groningen, the Netherlands) and the Royal Marsden Hospital (London, United Kingdom). Medical ethical committee approval was obtained in both institutions. All patients signed written informed consent. Consent for the ^{89}Zr-trastuzumab PET or ^{89}Zr-bevacizumab side studies was obtained

separately from consent for the clinical trial with NVP-AUY922 treatment.

Treatment

NVP-AUY922 was administered once a week intravenously at a starting dose of 70 mg/m^2 which was the recommended phase II dose in the first-in-human phase I trial with monotherapy NVP-AUY922 (29). As per protocol, doses were reduced to 54 mg/m^2 for significant adverse events, which were defined as $\geq$ grade 3 toxicity or grade 2 toxicity for at least 7 days. NVP-AUY922 was discontinued for any grade 4 toxicity.

Toxicity assessments

Patients were examined and assessed for adverse events weekly, and toxic effects were graded with the NCI CTCAE version 3.0. A complete blood and platelet count and serum chemistry panel measurement were repeated every week in the first 2 cycles, thereafter once every 2 weeks. After reports of visual symptoms in the phase I study, this trial required complete ophthalmologic assessment including testing for visual acuity, intraocular pressure, slit-lamp, dilated fundus, and color-vision. An additional electro retinogram was conducted. All ophthalmologic examinations were performed at baseline, when visual symptoms became present and at the end of cycle 2. Of note, 12-lead electrocardiograms were obtained at baseline and before and after every NVP-AUY922 infusion. The electrocardiograms were assessed for changes in QT duration. Patients were instructed to use loperamide as needed for diarrhea.

^{89}Zr-trastuzumab PET and ^{89}Zr-bevacizumab imaging

Patients with HER2-positive breast cancer, who consented to the ^{89}Zr-trastuzumab PET imaging side study, received 37 MBq/50 mg ^{89}Zr-trastuzumab intravenously. Production of clinical grade ^{89}Zr-trastuzumab was described previously (31). Each patient underwent a PET scan on days 2 and 4 postinjection. Two scan sequences were performed, with ^{89}Zr-trastuzumab injections at baseline and at day 15 of cycle 1. For patients with ER-positive breast cancer, who consented to the ^{89}Zr-bevacizumab PET imaging side study, a similar time frame was used after injection of 37 MBq/5 mg ^{89}Zr-bevacizumab. Clinical grade ^{89}Zr-bevacizumab was produced as described earlier (26). ^{89}Zr-trastuzumab and ^{89}Zr-bevacizumab distributions were scored visually and quantitatively by calculating the mean and maximum standardized uptake values ($SUV_{mean/max}$) at baseline and following NVP-AUY922 treatment (S.B.M. Gaykema and A.H. Brouwers). If >10 tumor lesions were visualized in one organ, then 10 were quantified. A high correlation was found between SUV_{mean} and SUV_{max} for healthy organs and tumor lesions (Pearson $r^2 = 0.99$ and $r^2 = 0.97$, respectively, $P < 0.0001$). Because it is less operator dependent, we present data as SUV_{max}. Response on ^{89}Zr-trastuzumab and ^{89}Zr-bevacizumab PET was compared with the response on CT after 8 weeks, only lesions of at least 1.0 cm were used to compare.

Pharmacodynamic markers

HSP70 and HER2-ECD were quantified by ELISA in PBMC and serum samples, respectively. PBMC samples were collected pretreatment and 5, 24, and 48 hours postdose and before infusion on day 8. Serum samples were collected at baseline, pretreatment at cycle 1 and 2 day 1, day 3, day 8, day 15, and every odd cycle.

Assessment of tumor response by CT and FDG-PET

Imaging included a CT scan of the chest, abdomen and pelvis, performed pretreatment and at the end of every even cycle. CT scans were assessed for tumor response by two independent radiologists according to RECIST1.0 criteria (30). All patients with a partial response (PR) or complete response (CR) were required to have confirmation of response performed $\geq$4 weeks after the criteria for response were first met. In case of stable disease (SD), follow-up measurements must have met SD criteria at least once after study entry at a minimum interval of 6 weeks. The best overall response was defined as the best response recorded from the start of the treatment until disease progression or withdrawal from the study. Clinical benefit rate was defined as CR+PR+SD. In a waterfall plot, best change in longitudinal tumor size will be presented. Whole body FDG-PET scans were performed at baseline and after 4 and 8 weeks. The acquisition protocol was standardized across sites. Patient needed to fast for approximately 6 hours before FDG-PET scanning. The patient was encouraged to maintain good hydration. Glucose levels were measured before the administration of FDG. The patient needed a blood glucose value of $\leq$200 mg/dL in order for the patient to have the FDG-PET. These scans were assessed per center by two independent nuclear medicine specialists blinded for clinical information. FDG-PET scans were assessed for new tumor lesions. In addition, up to five lesions with the highest uptake were identified on the baseline scans as index lesions. The index lesions were scored quantitatively by calculating the SUV_{max}. The percentage of change was subsequently calculated. The definitions for metabolic response were defined according to the European Organisation for Research and Treatment of Cancer, into a group with CR or PR (<−25%), a group with SD (−25% to +25%), and a group with progressive disease (>+25% and/or new tumor lesions; ref. 32). Response on FDG-PET was compared with the response on CT after 8 weeks, only lesions in the field of view of the CT and a size of at least 1.0 cm were used to compare.

Drug concentration measurements and pharmacokinetic assessment

Blood sampling to characterize pharmacokinetic was performed on cycle 1 day 1, immediately before NVP-AUY922 infusion, 5, 15, and 30 minutes during NVP-AUY922 infusion, immediately before the end of the infusion, at 5 minutes, 30 minutes, 1, 2, 4, 5, 8, 24, 48, and 72 hours postinfusion and before infusion on day

Table 1. Patient characteristics at study entry

	Patients with HER2-positive BC $n = 10$ (%)	Patients with ER-positive BC $n = 6$ (%)	All patients $n = 16$ (%)
Age, y (SD)	54.6 (10.5)	56.2 (9.0)	55.2 (9.7)
Predominant race, *n* (%)			
Caucasian	8 (80.0)	6 (100.0)	14 (87.5)
Black	1 (10.0)	0	1 (6.3)
Other	1 (10.0)	0	1 (6.3)
Body surface area, m^2 (SD)	1.9 (0.3)	1.8 (0.3)	1.8 (0.3)
LVEF (%; SD)	64.7 (11.1)	62.3 (6.8)	63.8 (9.5)
WHO performance status			
0	7 (70.0)	5 (83.3)	12 (75.0)
1	3 (30.0)	1 (16.7)	4 (25.0)
Tumor stage			
III	1 (10)	1 (16.7)	2 (12.7)
IV	9 (90)	5 (83.3)	14 (87.5)
Number of earlier regimens			
1	1	0	1
2	0	1	1
3	3	0	3
4	3	4	7
>4	3	1	4
Other	1	0	1

Abbreviation: LVEF, left ventricular ejection fraction.

8. The sample was centrifuged at a minimum of 1,500 *g* for 15 minutes and all plasma was transferred in tubes. An additional 2 mL of whole blood was obtained for plasma assay of NVP-AUY922 and its pharmacologically inactive metabolite BJP762 at the following time points: on cycle 1 day 1 at the end of the infusion, and then 1, 5, and 24 hours postinfusion. Because of the light sensitivity of NVP-AUY922 and its lack of stability in handling, all blood samples were protected from light during collection, handling, and processing and then stored at −70°C.

The blood and plasma samples collected were assayed for NVP-AUY922 and BJP762 concentrations by Novartis using a validated LC/MS-MS. Values below the lower limit of quantification of 0.8 ng/mL were reported as 0.00 ng/mL. Pharmacokinetic parameters were determined by noncompartmental method using WinNonlin Pro (Version 5.2).

Statistical analysis

All clinical data were collected by electronic data capture (Timaeus). Data are presented as mean ± SD and range. Statistical analysis was performed using a paired sampled *t* test for paired data. For correlation of the companion biomarker with RECIST 1.0, the Pearson test was used. The Kaplan–Meier method was used to estimate rates of progression over time and median times to progression (SPSS, version 19). All testing was two sided at the 5% level of significance.

Results

Patient characteristics

Sixteen patients were enrolled between February 2010 and July 2011. Baseline characteristics are summarized in Table 1. All patients have discontinued treatment (range 1–11 months), 13 (81%) because of radiological disease progression and two patients because of clinical progression (13%). One patient (6%) stopped treatment because of grade 2 nausea, which did not resolve after dose reduction.

Toxicity

The actual cumulative administered doses of NVP-AUY922 were lower than planned: 951.2 mg/m^2 versus 1175.4 mg/m^2. Eight patients required a dose reduction to 54 mg/m^2. Median time to reduction was 2.5 weeks (range 2–6). The most frequent adverse events (all grades, regardless of causality) were summarized in Supplementary Table S1. Nine serious adverse events occurred in 6 (37.5%) of the patients, none of which were suspected to be related to study drug. Scan procedures were uneventful, except in one case, in which the patient developed shivering, rigors, and bronchospasm after ^{89}Zr-trastuzumab administration. This was completely reversed within 10 minutes by hydrocortisone and chlorpheniramine administration, in line with a mild allergic reaction to trastuzumab. No more scan procedures with ^{89}Zr-trastuzumab were performed in this patient.

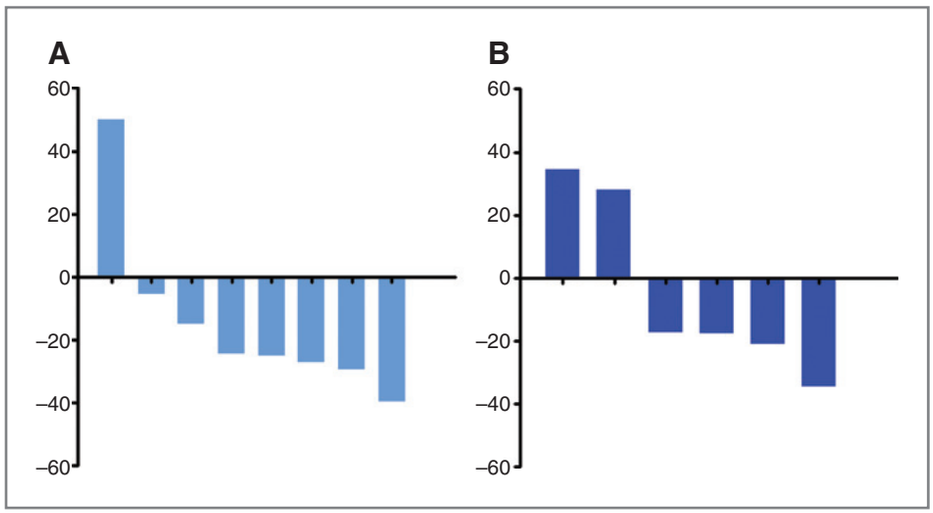

Figure 1. Maximal percentage change in SUV_{max} of target lesions on FDG-PET between baseline and after 3 weeks of treatment, in patients with HER2-positive (A) and ER-positive (B) breast cancer. Repeated FDG-PET could be performed in 8 of 10 patients with HER2-positive breast cancer, and in all of 6 patients with ER-positive breast cancer.

PET imaging

Repeated FDG-PET could be performed in 8 of 10 patients with HER2-positive breast cancer, and in all of 6 patients with ER-positive breast cancer. Best percentage change from baseline for FDG-PET SUV_{max} is shown graphically in Fig. 1. Partial metabolic response was seen in 5 patients, 4 with HER2-positive breast cancer and 1 with ER-positive breast cancer. Mean decrease in SUV_{max} on FDG-PET after 4 and 8 weeks was 12% ± 22% and 7% ± 30%, respectively ($P = 0.09$). Response on FDG-PET was not correlated with response on CT after 8 weeks ($r^2 = 0.18$; $P = 0.12$ at 4 weeks and $r^2 = 0.17$; $P = 0.13$ at 8 weeks).

Repeated ^{89}Zr-trastuzumab PET could be performed in 5 patients with HER2-positive disease, one patient only received the baseline scan. Twenty-nine lesions were visible on ^{89}Zr-trastuzmab PET. Visual analysis of PET imaging showed a time-dependent accumulation of ^{89}Zr-trastuzumab within the tumors at days 2 and 4 after ^{89}Zr-trastuzumab injection. The following analyses therefore reflect day 4 data from ^{89}Zr-trastuzumab PET at baseline and during

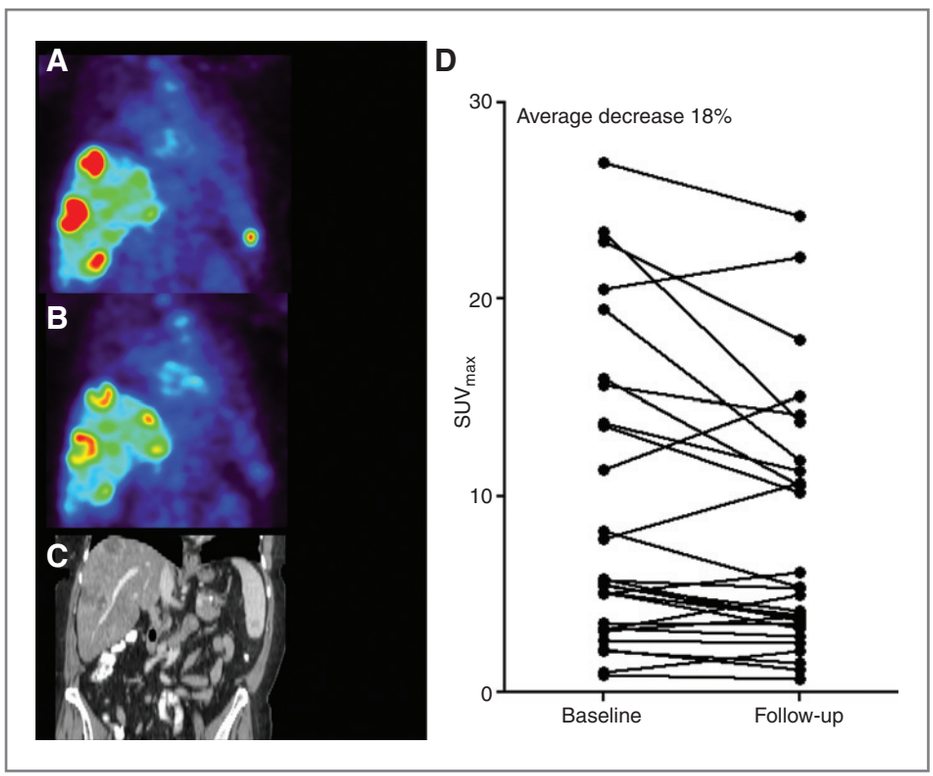

Figure 2. Representative coronal ^{89}Zr-trastuzumab PET images of a patient scanned before (A) and after (B) 3 weeks of treatment. Multiple liver lesions and one splenic lesion are shown. ^{89}Zr-trastuzumab PET could be performed in 6 of 10 HER2-positive patients, of which 5 underwent repeated scan procedures. The CT scan pretreatment is shown in C. D, a heterogeneous response in individual tumor lesions ($n = 29$) between baseline and follow-up, with an average decrease in SUV_{max} of 18%.

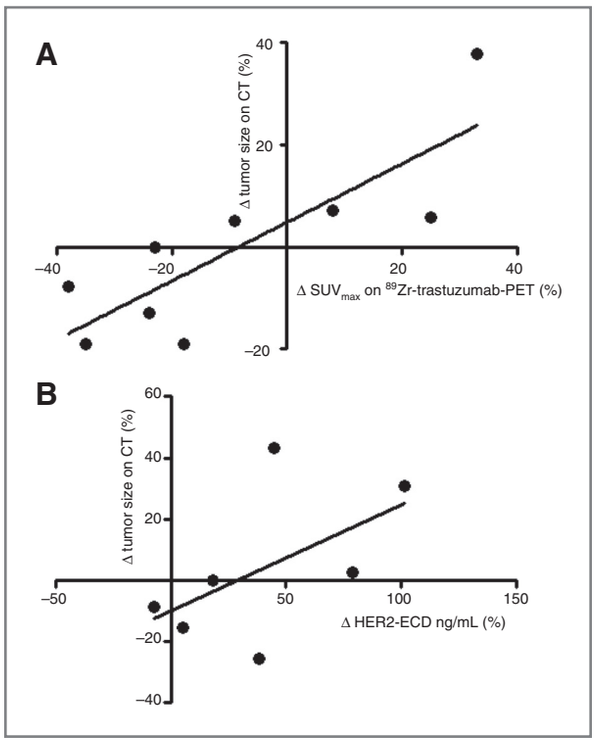

Figure 3. A, correlation of percentage change in SUV_{max} of ^{89}Zr-trastuzumab (*x*-axis) per lesion ($n = 9$) between baseline ^{89}Zr-trastuzumab-PET of 5 patients and after 3 weeks NVP-AUY922 treatment, and change in size of corresponding lesions on CT (*y*-axis) between baseline and after 8 weeks treatment with NVP-AUY922 (*y*-axis; $r^2 = 0.69$, $P = 0.0057$). B, correlation of maximal increase of HER2-ECD ($n = 6$) compared with baseline (*x*-axis), and change in size of CT in all target lesions of an individual patient (*y*-axis; $r^2 = 0.69$, $P = 0.02$).

treatment (the latter is now referred to as 3-week scan). Figure 2 shows a representative ^{89}Zr-trastuzumab PET. The mean SUV_{max} of ^{89}Zr-trastuzumab uptake at baseline was 9.0 ± 7.6 (0.9–26.9), decreasing during treatment to 7.8 ± 6.3 (range 0.7–24.2, $P = 0.047$). Heterogeneous treatment effect on SUV_{max} in the 29 individual tumor lesions was observed, both within and between patients (Fig. 2 and Supplementary Table S3). There was a correlation between the mean decrease in SUV on ^{89}Zr-trastuzumab PET scans after 3 weeks compared with baseline, and the change of size of tumor lesions on CT after 8 weeks of treatment compared with baseline ($r^2 = 0.69$, $P = 0.006$; Fig. 3).

Of patients with ER-positive breast cancer, 5 underwent a repeated ^{89}Zr-bevacizumab PET scan, one patient only received the baseline scan. Visual analysis of PET imaging at days 2 and 4 posttracer injection showed a time-dependent accumulation of ^{89}Zr-bevacizumab within the tumor lesions, with on day 4 a 1.12-fold higher ^{89}Zr-bevacizumab tumor uptake compared with day 2. The following analyses therefore reflect day 4 data from ^{89}Zr-bevacizumab PET at baseline and during treatment. Figure 4 shows a representative ^{89}Zr-bevacizumab-PET. SUV_{max} on the day 4 scan at baseline was 2.3 ± 1.1 (range 0.9–5.2) which was unaffected during treatment with 2.4 ± 1.4 (range 0.6–6.6; $P = 0.56$). Because of a high physiologic liver uptake of ^{89}Zr-bevacizumab, liver lesions could not be visualized, except for two patients in whom the liver metastases were not accumulating ^{89}Zr-bevacizumab, therefore leaving a "cold" spot that could be visualized. Twenty-three lesions at baseline were detected in 5 patients, 20 of them were bone lesions that were also detected on FDG-PET, but not measurable on CT (Supplementary Table S4).

Biomarkers

At baseline, measurement of HSP70 levels in PMBCs was performed in 15 patients. Median HSP70 levels were 29.0 ng/mg (range 10.0–69.1). Between baseline and follow-up measurements, the medium of all maximal HSP70 increases in PBMCs in these patients was 359.4% ± 350.5. The induction in HSP70 confirmed target inhibition defined in a previous phase I study (29). A higher baseline level of HER2-ECD was correlated with a larger tumor size decrease on CT (Pearson $r^2 = 0.60$; $P = 0.025$). The median of maximal HER2-ECD increase was 13.6% ± 33.4%, which was also positively correlated with tumor size decrease after 8 weeks of treatment (Pearson $r^2 = 0.69$; $P = 0.020$).

Efficacy

One patient with HER2-positive breast cancer experienced a confirmed PR after 8 weeks. An additional 7 patients (3 with HER2-positive breast cancer and 4 with ER-positive breast cancer) experienced confirmed SD (Supplementary Table S2), resulting in a disease control rate of 50% (95% confidence interval, 24.7%–75.3%). Median time to progression was 3 months (range 1–10). Five patients experienced time-to-progression >6 months. A waterfall plot of best responses on CT showed a decrease of mean tumor size in most patients (Fig. 5).

Pharmacokinetics

Supplementary Figure S1 shows mean blood concentration-time profiles for NVP-AUY922 (A) and its metabolite BJP762 (B). Following the initial rapid decline in concentration levels after the infusion, NVP-AUY922 was eliminated slowly with a flat terminal phase half-life of 120 hours (range 54–404). AUC from time zero until the last measurable samples was $7.7 \times 10^3 \pm 2.5 \times 10^3$ and $4.5 \times 10^3 \pm 2.0 \times 10^3$ for, respectively, AUY922 and BJP762 in the HER2 group and $9.9 \times 10^3 \pm 2.6 \times 10^3$ and $1.3 \times 10^4 \pm 2.1 \times 10^4$ for, respectively, AUY922 and BJP762 in the ER group. Peak concentrations were observed at the end of infusion for both NVP-AUY922 and BJP762, suggesting the rapid biotransformation from NVP-AUY922 to BJP762 *in vivo*. It should be noted that whole blood AUY922 is measured, including the fraction encapsulated in red blood cells (which is not available for metabolization); this makes the apparent half-life longer for parent AUY922 as compared with its metabolite BJP762. These results were in line with

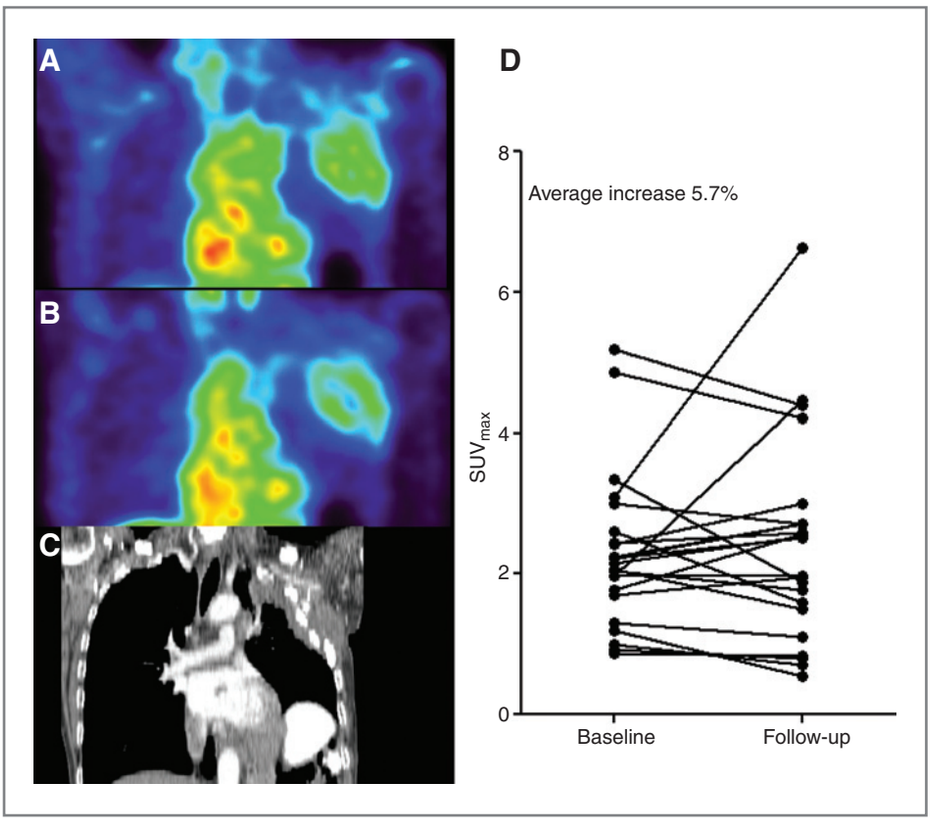

Figure 4. Representative coronal ^{89}Zr-bevacizumab PET images of a patient scanned before (A) and after (B) 3 weeks of treatment. The patient had a large tumor mass in the chest wall. ^{89}Zr-bevacizumab PET could be performed in 6 of 10 patients of which 5 underwent repeated scan procedures. The CT scan pretreatment is shown in C. D, a heterogeneous response in individual tumor lesions ($n = 23$) between baseline and follow-up, with an average increase of SUV_{max} of 5.7%.

the findings in the first in-human phase I and ongoing phase II studies (29, 33).

Discussion

This study provides early evidence that the change between tumor uptake on baseline and early ^{89}Zr-trastuzumab PET after 3 weeks of treatment with HSP90 inhibitor NVP-AUY922 had a moderate positive correlation with change in tumor size on CT after 8 weeks of treatment. In contrast, early FDG-PET, performed after 4 weeks of treatment, did not correlate with change in tumor size on the 8 week CT.

In a preclinical model, ^{18}F-FDG uptake was minimally affected by NVP-AUY922 administered to a spheroid model with BT474 breast cancer cells (34). Previously, 17AAG effect could be visualized *in vivo* by reduced radiolabeled trastuzumab uptake, but not by means of FDG-PET (24). These results all support that more specific imaging of targets is more useful to assess the effects of HSP90 inhibition. In human tumor-bearing mice, we showed that HER2 and VEGF downregulation could be visualized after treatment with an HSP90 inhibitor (22, 23). Now also in the clinical setting, we observed that novel PET probes such as ^{89}Zr-trastuzumab can potentially be used to provide whole body insights into response of HER2-amplified breast cancer to NVP-AUY922. Interestingly, we found a heterogeneous effect on the SUV_{max}, within tumor lesions, both within and between patients. This effect was in line with both heterogeneous intra- and inter-patient tumor responses on CT. A further application of ^{89}Zr-trastuzumab PET could be predefining areas of tumor that are not responding to targeted treatment with HSP90 inhibitors such as NVP-AUY922. Biopsying such areas would provide valuable insights in the biology of HSP90 resistance in the tumor. In addition, interlesional heterogeneity of gene expression is increasingly recognized as a relevant factor which is likely to affect treatment response (35, 36). The precise clinical implications of *in vivo* heterogeneity of HER2 expression are currently further investigated in the Dutch multicenter IMPACT breast trial (Trial Registration ID: NCT01832051). With regard to the use of ^{89}Zr-trastuzumab- or ^{89}Zr-bevacizumab PET, it should be taken into account that not much is known about reproducibility of the scans in patients with cancer. However, a test-retest set up for this type of scan requires an interval of at least 2 weeks because of the particularly long half-life of ^{89}Zr-tracers. Such an interval would require otherwise stable conditions, which is not typically the case in patients with metastatic cancer. As a result, variation in measurements can also be induced by a factor such as tumor growth. In addition, the often necessary start of systemic treatment in (rapidly) progressive disease would induce further variability. In a preclinical study, there was no significant difference in uptake of ^{89}Zr-trastuzumab-F(ab′)$_2$ in SKBR3 tumor-bearing mice without treatment (interval between two scans 7 days; ref. 37).

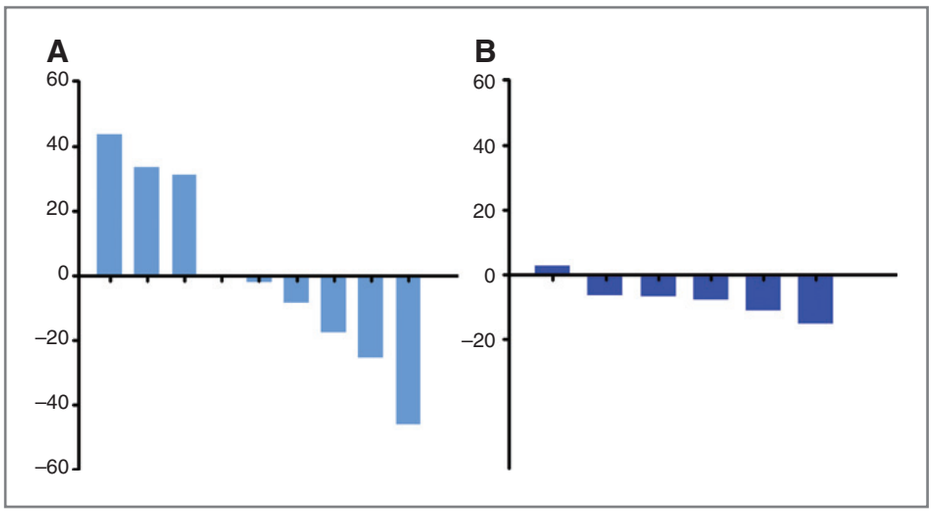

Figure 5. Maximal percentage change in sum of longitudinal axis of target lesions on CT, between baseline and 8 weeks of treatment in patients with HER2-positive (A) and ER-positive (B) breast cancer. Repeated CT was performed in 9 of 10 patients with HER2-positive breast cancer and in all 6 patients with ER-positive breast cancer.

We did not find a correlation between uptake change on ^{89}Zr-bevacizumab PET and CT. This could be due to the fact that most lesions found on ^{89}Zr-bevacizumab PET were bone lesions that were not measurable on CT. Another potentially contributing factor is that HIF1α is likely a less prominent client protein of HSP90 than HER2 (38). HSP90 can influence angiogenesis in multiple ways, including degradation of HIF1α, which drives production of VEGF or degradation of VEGF receptor. Although angiogenesis is a hallmark of cancer (39), inhibition of angiogenesis is less critical to response to treatment of breast cancer as evidenced by an increasing number of studies showing no clinical benefit of bevacizumab in breast cancer (40, 41). Moreover in breast tumors, ^{89}Zr-bevacizumab uptake was consistently lower than in renal cell cancer (25, 27). In view of this, the fact that ER itself is influenced by HSP90 inhibition, and that it is now possible to visualize ER on tumor lesions by means of whole body ^{18}Fluorestradiol (FES) PET, it would be of great interest to use FES-PET in patients with ER-positive breast cancer receiving HSP90 inhibition. However, at time of design of this study, FES was not clinically available in our clinic. Therefore, although ^{89}Zr-bevacizumab PET cannot be used to assess treatment response, a recent clinical study in patients with breast cancer indicated that it may be of use in the setting of primary tumor detection (27). In addition, in patients with HER2-positive metastatic breast cancer, HER2-ECD at baseline and decrease during treatment, positively correlated with tumor response. This is in line with a previous trial, in which HER2-ECD also correlated to trastuzumab and paclitaxel response (28). Pharmacodynamic markers such as HSP70 induction and pharmacokinetic parameters confirmed pharmacokinetic and pharmacodynamic findings observed in a previous phase I study (29).

In the present trial, we found an encouraging clinical benefit rate of 50% in heavily pretreated patients with breast cancer with progressive disease at start of treatment. Studies with first generation HSP90 inhibitors only demonstrated modest clinical benefit in HER2-amplified breast cancer (30); however, in this trial, the clinical benefit was also seen in ER-positive breast cancer. NVP-AUY922 is currently further evaluated in combination with trastuzumab and has shown encouraging results in a phase II study (17). In light of our results, it would also be of interest to further evaluate HSP90 inhibition for the treatment of ER-positive metastatic breast cancer, particularly because the ER itself is a client protein of HSP90.

Concluding, in this clinical trial in patients with advanced HER2- or ER-positive metastatic breast cancer, effect of treatment with HSP90 inhibitor NVP-AUY922, on *in vivo* degradation of HER2 and VEGF was assessed with ^{89}Zr-trastuzumab PET or ^{89}Zr-bevacizumab PET. ^{89}Zr-trastuzumab PET results at 3 weeks positively correlated with CT responses in individual lesions. Thus, novel PET probes such as ^{89}Zr-trastuzumab might provide insights into responses to novel agents active in HER2-amplified breast cancer, such as NVP-AUY922. This finding should be assessed in further, larger studies.

Disclosure of Potential Conflicts of Interest

M. Akimov is an employee of and has ownership interest (including patents) in Novartis. U. Banerji reports receiving a commercial research grant from and is a consultant/advisory board member for Novartis. No potential conflicts of interest were disclosed by the other authors.

Authors' Contributions

Conception and design: C.P. Schroder, J. Vitfell-Rasmussen, S. Chua, T.H. Oude Munnink, M.N. Lub-de Hooge, E.G.E. de Vries, U. Banerji
Development of methodology: C.P. Schroder, S. Chua, T.H. Oude Munnink, A.H. Brouwers, M. Akimov, M.N. Lub-de Hooge, E.G.E. de Vries
Acquisition of data (provided animals, acquired and managed patients, provided facilities, etc.): S.B.M. Gaykema, C.P. Schroder, J. Vitfell-Rasmussen, S. Chua, T.H. Oude Munnink, A.H. Brouwers, A.H.H. Bongaerts, M. Akimov, M.N. Lub-de Hooge, E.G.E. de Vries, U. Banerji
Analysis and interpretation of data (e.g., statistical analysis, biostatistics, computational analysis): S.B.M. Gaykema, C.P. Schroder, S. Chua,

T.H. Oude Munnink, A.H. Brouwers, A.H.H. Bongaerts, M. Akimov, E.G.E. de Vries, U. Banerji

Writing, review, and/or revision of the manuscript: S.B.M. Gaykema, C.P. Schroder, J. Vitfell-Rasmussen, S. Chua, T.H. Oude Munnink, A.H. Brouwers, A.H.H. Bongaerts, M. Akimov, C. Fernandez-Ibarra, M.N. Lub-de Hooge, E.G.E. de Vries, C. Swanton, U. Banerji

Administrative, technical, or material support (i.e., reporting or organizing data, constructing databases): S.B.M. Gaykema, C.P. Schroder, J. Vitfell-Rasmussen, S. Chua, M. Akimov, C. Fernandez-Ibarra

Study supervision: C.P. Schroder, J. Vitfell-Rasmussen, A.H. Brouwers, M. Akimov, C. Fernandez-Ibarra, E.G.E. de Vries, U. Banerji

Acknowledgments

The authors thank J.R. de Jong, H.H. Nienhuis, G. Sieling, and L. Pot for assistance. This clinical trial was in part designed at the 2007 ECCO–AACR–ASCO 9th Workshop: Methods in Clinical Cancer Research (Flims, Switzerland by C.P. Schröder).

Grant Support

This work was supported by Novartis, The American Women's Club of the Hague KP565404 (2008), and grants RUG 2007-3739 and RUG 2009-4273 of the Dutch Cancer Society. The UK investigators acknowledge infrastructural grants, including NIHR grants to The Institute of Cancer Research/The Royal Marsden NHS Foundation Trust, the Breast Cancer Research Foundation, Experimental Cancer Medicine Centre grants (C51/A7401/C12540/A15573), infrastructural grant support of Cancer Research UK grants (C309/A8274/A309/A11566; C51/A6883), and NIHR Biomedical Research Centre funding.

The costs of publication of this article were defrayed in part by the payment of page charges. This article must therefore be hereby marked *advertisement* in accordance with 18 U.S.C. Section 1734 solely to indicate this fact.

Received February 27, 2014; revised May 5, 2014; accepted May 14, 2014; published online August 1, 2014.

References

1. Chia SK, Speers CH, D'yachkova Y, Kang A, Malfair-Taylor S, Barnett J, et al. The impact of new chemotherapeutic and hormone agents on survival in a population-based cohort of women with metastatic breast cancer. Cancer 2007;110:973–9.
2. Gennari A, Conte P, Rosso R, Orlandini C, Bruzzi P. Survival of metastatic breast carcinoma patients over a 20-year period: a retrospective analysis based on individual patient data from six consecutive studies. Cancer 2005;104:1742–50.
3. Banerji U. Heat shock protein 90 as a drug target: some like it hot. Clin Cancer Res 2009;15:9–14.
4. Banerji U, Walton M, Raynaud F, Grimshaw R, Kelland L, Valenti M, et al. Pharmacokinetic-pharmacodynamic relationships for the heat shock protein 90 molecular chaperone inhibitor 17-allylamino, 17-demethoxygeldanamycin in human ovarian cancer xenograft models. Clin Cancer Res 2005;11:7023–32.
5. Bagatell R, Khan O, Paine-Murrieta G, Taylor CW, Akinaga S, Whitesell L. Destabilization of steroid receptors by heat shock protein 90-binding drugs: a ligand-independent approach to hormonal therapy of breast cancer. Clin Cancer Res 2001;7:2076–84.
6. Lee MO, Kim EO, Kwon HJ, Kim YM, Kang HJ, Kang H, et al. Radicicol represses the transcriptional function of the estrogen receptor by suppressing the stabilization of the receptor by heat shock protein 90. Mol Cell Endocrinol 2002;188:47–54.
7. Wainberg ZA, Anghel A, Rogers AM, Desai AJ, Kalous O, Conklin D, et al. Inhibition of HSP90 with AUY922 induces synergy in HER2-amplified trastuzumab-resistant breast and gastric cancer. Mol Cancer Ther 2013;12:509–19.
8. Eccles SA, Massey A, Raynaud FI, Sharp SY, Box G, Valenti M, et al. NVP-AUY922: a novel heat shock protein 90 inhibitor active against xenograft tumor growth, angiogenesis, and metastasis. Cancer Res 2008;68:2850–60.
9. Forsythe JA, Jiang BH, Iyer NV, Agani F, Leung SW, Koos RD, et al. Activation of vascular endothelial growth factor gene transcription by hypoxia-inducible factor 1. Mol Cell Biol 1996;16:4604–13.
10. Ferrarini M, Heltai S, Zocchi MR, Rugarli C. Unusual expression and localization of heat-shock proteins in human tumor cells. Int J Cancer 1992;51:613–9.
11. Kamal A, Thao L, Sensintaffar J, Zhang L, Boehm MF, Fritz LC, et al. A high-affinity conformation of Hsp90 confers tumour selectivity on Hsp90 inhibitors. Nature 2003;425:407–10.
12. Brough PA, Aherne W, Barril X, Borgognoni J, Boxall K, Cansfield JE, et al. 4,5-diarylisoxazole Hsp90 chaperone inhibitors: potential therapeutic agents for the treatment of cancer. J Med Chem 2008;51:196–218.
13. Jensen MR, Schoepfer J, Radimerski T, Massey A, Guy CT, Brueggen J, et al. NVP-AUY922: a small molecule HSP90 inhibitor with potent antitumor activity in preclinical breast cancer models. Breast Cancer Res 2008;10:R33.
14. Sequist LV, Gettinger S, Senzer NN, Martins RG, Janne PA, Lilenbaum R, et al. Activity of IPI-504, a novel heat-shock protein 90 inhibitor, in patients with molecularly defined non-small-cell lung cancer. J Clin Oncol 2010;28:4953–60.
15. Pacey S, Wilson RH, Walton M, Eatock MM, Hardcastle A, Zetterlund A, et al. A phase I study of the heat shock protein 90 inhibitor alvespimycin (17-DMAG) given intravenously to patients with advanced solid tumors. Clin Cancer Res 2011;17:1561–70.
16. Modi S, Stopeck AT, Linden HM, Solit DB, Chandarlapaty S, Rosen N, et al. HSP90 inhibition is effective in breast cancer: a phase 2 trial of tanespimycin (17AAG) plus trastuzumab in patients with HER2-positive metastatic breast cancer progressing on trastuzumab. Clin Cancer Res 2011;7:5132–9.
17. Kong A. Phase IB/II study of the HSP90 inhibitor AUY922, in combination with trastuzumab, in patients with HER2+ advanced breast cancer. J Clin Oncol 30, 2012 (suppl; abstr 530).
18. Friedberg JW, Chengazi V. PET scans in the staging of lymphoma: current status. Oncologist 2003;8:438–47.
19. Torizuka T, Nakamura F, Kanno T, Futatsubashi M, Yoshikawa E, Okada H, et al. Early therapy monitoring with FDG-PET in aggressive non-Hodgkin's lymphoma and Hodgkin's lymphoma. Eur J Nucl Med Mol Imaging 2004;31:22–8.
20. Weber WA. Use of PET for monitoring cancer therapy and for predicting outcome. J Nucl Med 2005;46:983–95.
21. Kelloff GJ, Hoffman JM, Johnson B, Scher HI, Siegel BA, Cheng EY, et al. Progress and promise of FDG-PET imaging for cancer patient management and oncologic drug development. Clin Cancer Res 2005;11:2785–808.
22. Oude Munnink TH, Korte MA, Nagengast WB, Timmer-Bosscha H, Schroder CP, Jong JR, et al. ^{89}Zr-trastuzumab PET visualises HER2 downregulation by the HSP90 inhibitor NVP-AUY922 in a human tumour xenograft. Eur J Cancer 2010;46:678–84.
23. Nagengast WB, de Korte MA, Oude Munnink TH, Timmer-Bosscha H, den Dunnen WF, Hollema H, et al. ^{89}Zr-bevacizumab PET of early antiangiogenic tumor response to treatment with HSP90 inhibitor NVP-AUY922. J Nucl Med 2010;51:761–7.
24. Smith-Jones PM, Solit D, Afroze F, Rosen N, Larson SM. Early tumor response to Hsp90 therapy using HER2 PET: comparison with ^{18}F-FDG PET. J Nucl Med 2006;47:793–6.
25. Oosting SF, Brouwers AH, Van Es SC, Nagengast WB, Oude Munnink TH, Hooge MN, et al. ^{89}Zr-bevacizumab PET imaging in metastatic renal cell carcinoma patients before and during antiangiogenic treatment. J Clin Oncol 30, 2012(suppl; abstr 10581).
26. Dijkers EC, Oude Munnink TH, Kosterink JG, Brouwers AH, Jager PL, de Jong JR, et al. Biodistribution of ^{89}Zr-trastuzumab and PET imaging of HER2-positive lesions in patients with metastatic breast cancer. Clin Pharmacol Ther 2010;87:586–92.
27. Gaykema SB, Brouwers AH, Lub-de Hooge MN, Pleijhuis RG, Timmer-Bosscha H, Pot L, et al. ^{89}Zr-bevacizumab PET imaging in primary breast cancer. J Nucl Med 2013;54:1014–8.
28. Fornier MN, Seidman AD, Schwartz MK, Ghani F, Thiel R, Norton L, et al. Serum HER2 extracellular domain in metastatic breast cancer

patients treated with weekly trastuzumab and paclitaxel: association with HER2 status by immunohistochemistry and fluorescence in situ hybridization and with response rate. Ann Oncol 2005; 16:234–9.
29. Sessa C, Shapiro GI, Bhalla KN, Britten C, Jacks KS, Mita M, et al. First-in-human phase I dose-escalation study of the HSP90 inhibitor AUY922 in patients with advanced solid tumors. Clin Cancer Res 2013;19:3671–80.
30. Therasse P, Arbuck SG, Eisenhauer EA, Wanders J, Kaplan RS, Rubinstein L, et al. New guidelines to evaluate the response to treatment in solid tumors. European Organization for Research and Treatment of Cancer, National Cancer Institute of The United States, National Cancer Institute of Canada. J Natl Cancer Inst 2000;92: 205–16.
31. Dijkers EC, Kosterink JG, Rademaker AP, Perk LR, van Dongen GA, Bart J, et al. Development and characterization of clinical-grade ^{89}Zr-trastuzumab for HER2/neu immunoPET imaging. J Nucl Med 2009; 50:974–81.
32. Young H, Baum R, Cremerius U, Herholz K, Hoekstra O, Lammertsma AA, et al. Measurement of clinical and subclinical tumour response using [18F]-fluorodeoxyglucose and positron emission tomography: Review and 1999 EORTC recommendations. European Organization for Research and Treatment of Cancer (EORTC) PET study group. Eur J Cancer 1999;35:1773–82.
33. Schröder CP, Pedersen JV, Chua S, Swanton C, Akimov M, Ide S, et al. Use of biomarkers and imaging to evaluate the treatment effect of AUY922, an HSP90 inhibitor, in patients with HER2+ or ER+ metastatic breast cancer. J Clin Oncol 29: 2011 (suppl; abstr e11024).
34. Bergstrom M, Monazzam A, Razifar P, Ide S, Josephsson R, Langstrom B. Modeling spheroid growth, PET tracer uptake, and treatment effects of the Hsp90 inhibitor NVP-AUY922. J Nucl Med 2008; 49:1204–10.
35. Hanna WM, Ruschoff J, Bilous M, Coudry RA, Dowsett M, Osamura RY, et al. HER2 in situ hybridization in breast cancer: clinical implications of polysomy 17 and genetic heterogeneity. Mod Pathol 2014; 27:4–18.
36. Gerlinger M, Rowan AJ, Horswell S, Larkin J, Endesfelder D, Gronroos E, et al. Intratumor heterogeneity and branched evolution revealed by multiregion sequencing. N Engl J Med 2012;366:883–92.
37. Oude Munnink TH, de Vries EG, Vedelaar SR, Timmer-Bosscha H, Schroder CP, Brouwers AH, et al. Lapatinib and 17AAG reduce ^{89}Zr-trastuzumab-F(ab′)2 uptake in SKBR3 tumor xenografts. Mol Pharm 2012;9:2995–3002.
38. Sain N, Krishnan B, Ormerod MG, De Rienzo A, Liu WM, Kaye SB, et al. Potentiation of paclitaxel activity by the HSP90 inhibitor 17-allylamino-17-demethoxygeldanamycin in human ovarian carcinoma cell lines with high levels of activated AKT. Mol Cancer Ther 2006;5:1197–208.
39. Hanahan D, Weinberg RA. Hallmarks of cancer: the next generation. Cell 2011;144:646–74.
40. Brufsky AM, Hurvitz S, Perez E, Swamy R, Valero V, O'Neill V, et al. RIBBON-2: a randomized, double-blind, placebo-controlled, phase III trial evaluating the efficacy and safety of bevacizumab in combination with chemotherapy for second-line treatment of human epidermal growth factor receptor 2-negative metastatic breast cancer. J Clin Oncol 2011;29:4286–93.
41. Robert NJ, Dieras V, Glaspy J, Brufsky AM, Bondarenko I, Lipatov ON, et al. RIBBON-1: randomized, double-blind, placebo-controlled, phase III trial of chemotherapy with or without bevacizumab for first-line treatment of human epidermal growth factor receptor 2-negative, locally recurrent or metastatic breast cancer. J Clin Oncol 2011;29:1252–60.